The Effect of the Extrusion Temperature on the Recrystallization Textures of an Extruded AA6005C Alloy

Dr. Kentaro IHARA[*1], **Takahiro SHIKAMA**[*2], **Keiji MORITA**[*3]
[*1] Technology Control Dept. Moka Plant, Aluminum & Copper Business
[*2] Aluminum Extrusion & Fabrication Plant, Chofu Works, Aluminum & Copper Business
[*3] SHINKO FAB TECH, LTD.

A study was conducted to determine the effect of the extrusion temperature on the recrystallized grain size and texture of an AA6005C alloy. Several extrusion tests were conducted at temperatures from 753 to 793K at an extrusion speed of 3m/min. A decrease in extrusion temperature from 793K to 753K was found to increase the average size of recrystallized grains from 170μm to 230μm and the volume fraction of cube-oriented recrystallized grains from 30% to 40%. A high-temperature compression test, conducted to elucidate the process of recrystallized grain formation, revealed that, compared with extrusion at 793K, extrusion at 753K yields fewer recrystallized grains immediately after the deformation, indicating that a larger amount of energy is stored in the un-recrystallized region. The increased stored energy is considered to have promoted the preferential growth of the recrystallized Cube grains.

Introduction

The 6000 series Al-Mg-Si alloys are used as extrusions mainly in the fields of transportation equipment, building materials and electronic equipment. The structural materials for transportation equipment, including automobiles, are required to have properties such as mechanical strength, corrosion resistance and weldability[1]. Generally, these materials are forcibly cooled after extrusion, aged at high temperatures to a T5 condition and used in the high strength condition with their fibrous structures extending in the extrusion direction. The mechanical properties of an extruded material depend on its recrystallization texture. For example, the texture, highly oriented in the Cube direction, {100} <001>, of a hollow profile is reported to improve impact resistance[2]. The report that the recrystallization texture of an extruded material depends on the extrusion temperature is based primarily on round bars[3], and not much has been reported concerning hollow profiles. This study aims to clarify the effect of the extrusion conditions on the formation process of the recrystallization texture in a hollow profile of AA6005C (JIS 6N01)-T5 aluminum alloy. A study was conducted on the recrystallization textures of the hollow profiles, extruded at various temperatures and T5 treated. The following is an outline of the study.

1. Experimental method

The tested samples were prepared from hollow profiles made of an AA6005C (JIS 6N01)-T5. Their chemical composition and the process of producing the samples are shown **Table 1** and **Fig. 1**, respectively. Each billet, having a diameter of φ155mm, was homogenized at 520℃ for 4h, reheated to a temperature of 480℃, 500℃, or 520℃, and hot-extruded at a rate of 3m/min with an extrusion ratio of 44. The extrusion exit temperature was approximately 15℃ higher than the reheating temperature, due to the heat of deformation. The extruded profiles were held for 20s after the extrusion and then water cooled. They were subsequently aged at 190℃ for 3h to prepare the T5 treated samples.

These samples were subjected to tensile tests,

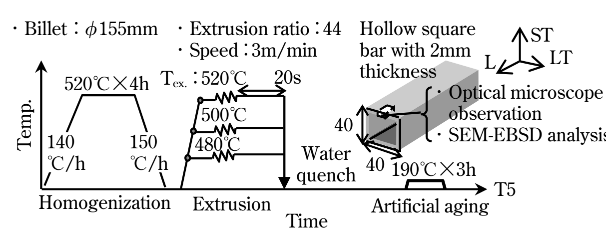

Fig. 1 Schematic view of the process for extruded 6005C alloys

Table 1 Chemical composition of studied Al-Mg-Si alloy (wt%)

	Si	Fe	Cu	Mn	Mg	Cr	Zn	Ti	Mn+Cr	Unspecified other elements	
										Each	Total
Specimen	0.40	0.20	0.15	—	0.80	—	—	0.02	—	—	—
AA6005C	0.40−0.90	0.35	0.35	0.50	0.40−0.80	0.30	0.25	0.10	≦0.50	0.05	0.15

optical microscopy observation, texture measurement and transmission electron microscopy (TEM) observation. Each tensile test was performed on a JIS13B specimen with its longitudinal direction parallel to the extrusion direction (L direction); the specimens each having a gauge length of 50mm. The tensile tests were conducted at a cross head speed of 2mm/min and at an initial strain rate of $7\times10^{-4}s^{-1}$. The crystal grain structures were observed under an optical microscope on the LT-ST cross sections of the samples etched by 5% sodium hydroxide. The texture measurement was conducted according to the electron back scattering pattern (EBSP) method using a scanning electron microscope (SEM). An LT-ST cross-section of each sample was electro-polished and was measured by an orientation imaging microscope (OIM), manufactured by TSL Solutions, that is mounted on an SEM (JEOL6500F), made by Japan Electro Optical Laboratory. The acceleration voltage was 15kV, and an area of 2×2mm was measured with a step interval of 5μm. The TEM observation was conducted to measure the size of disperse particles and their spacing. In addition to the extrusion test, elevated temperature compression tests were conducted on the sample billets to clarify the initial formation process of the recrystallized structure. **Fig. 2** schematically depicts the testing conditions. Column shaped specimens, each having a dimension of ϕ8×12mm, were machined from the billet homogenized at 520℃ for 4h. These specimens were subjected to the compression test at a strain rate of $10s^{-1}$ and a compression ratio of 75%. These high temperature compression tests were performed at the temperatures of 495℃ and 535℃, 15℃ higher than the respective extrusion temperatures of 480℃ and 520℃. This was to account for the deformation heat generated during the extrusion. The test employed the THERMECMASTOR-Z, made by Fuji Electronic Industrial Co., Ltd. After completing the deformation by compression, the samples were held for 2 and 5 seconds, respectively, before being water cooled. Then the microstructure at the center of each sample was observed on a section parallel to the compression axis, using the optical microscope and SEM-EBSD.

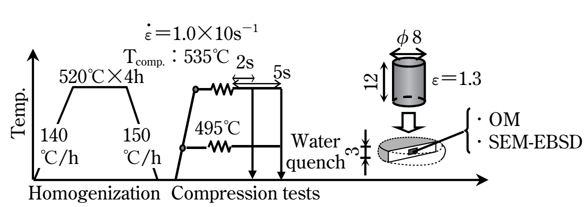

Fig. 2 Schematic view of the process of hot compression tests

2. Experimental results

2.1 The tensile properties of the samples

The tensile properties in the extrusion direction of the sample, shown in **Table 2**, satisfy the requirements of JIS H4100 with a tensile strength and proof strength slightly higher than the standard values. The tensile strength and proof strength decreased with decreasing extrusion temperature.

2.2 The microstructures of the samples

2.2.1 Crystal grain structure

Fig. 3 shows the optical micrographs of the recrystallization structures of the samples. **Table 3** summarizes the results of the microstructure measurements performed on the materials extruded at various temperatures. For extrusion temperatures ranging from 480 to 520℃, the recrystallization occurred throughout the wall thickness. When the extrusion temperature was lowered from 520℃ to 480℃, the average size of the recrystallized grain in

Table 2 Tensile properties of extruded 6005C-T5 specimens

$T_{ex.}$ (℃)		TS (MPa)	YS (MPa)	El. (%)
520		278	255	12
500		277	252	12
480		266	241	12
Standard data of 6005C [12]	T5	265	225	14
JIS H4100	T5	≧245	≧205	≧8

Table 3 Summary of the measurement results

$T_{ex.}$ (℃)		480	500	520
Mean grain size (μm)	Surface layer	132	139	136
	Center layer	234	178	165
Area fraction of texture (%) (LT-ST cross section)	Cube	38	30	29
	Goss	8	8	9
	Brass	4	3	5
	S	3	2	6
	Cu	3	1	2
	{112}<110>	3	2	2
	{001}<110>	3	1	1
Mean dispersoids size (nm)		140	136	140
Mean dispersoids space (μm)		2.2	2.5	2.2

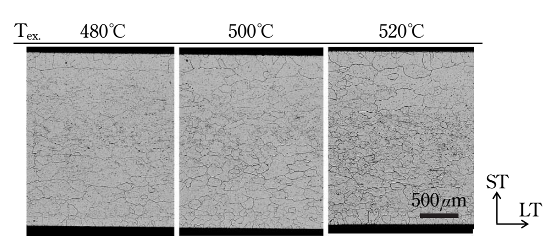

Fig. 3 Optical microstructure of extruded 6005C-T5 alloys (Tex.: Extrusion temperature)

the center layer increased from 165 μm to 234 μm.

2.2.2 Crystal orientation distribution

Fig. 4 shows the crystal orientation distributions of the samples. Fig. 4 (A) is an inverse pole figure map showing the crystal orientation in the L-direction, with the orientations depicted by the color inside the stereographic triangle in the right hand side of the figure. Fig. 4 (B) is a color depiction of the distribution of the major texture orientations, i.e., the Cube orientation {001} <100>, Goss orientation {001} <100>, Brass orientation {011} <211>, S orientation {123} <634>, Cu orientation {112} <111>, {112} <110> orientation and {001} <110> orientation. The black solid lines in Fig. 4 (B) indicate boundaries with a misorientation of 15° or greater. These boundaries correspond to high-angle grain boundaries.

As shown in Fig. 4 (A), the center layer has a crystal orientation distribution that is different from that of the surface layer. The center layer has a structure oriented in the <001> direction, while the surface layer has an orientation distribution that is relatively random. The center layer is primarily dominated by the distribution of the Cube orientation, and subsequently dominated by the Goss orientation. In the surface layer, the {112} <110> orientation and {001} <110> orientation are distributed, but these orientations are non-existent in the center layer. These are the orientations that are the same as the ones[3)-5)] formed by the shear strain imposed on the extrusion surfaces. Also observed in the surface layer are the distributions of the Goss orientation, Brass orientation, S orientation and Cu orientation.

The center layer was separated from the surface layer on the basis of the difference in the crystal orientation distribution shown in Fig. 4 (A). For each of these layers, the recrystallized grain size was measured from the average spacing of high-angle grain boundaries. The result is shown in **Fig. 5**. When the extrusion temperature was lowered from 520℃ to 480℃, the recrystallized grain size in the center layer increased from 165 μm to 234 μm. On the other hand, the recrystallized grain size in the surface layer remained in the range from 136 μm to 132 μm, showing little if any change. **Fig. 6** shows the relationship between the area fractions of the oriented grains and the extrusion temperature. The area fractions of the oriented grains were measured throughout the wall thickness in Fig. 4 (B). The major oriented grains, whose area fractions are affected by the extrusion temperature, are the Cube-oriented grains distributed in the center layer. The area fraction of the Cube-oriented grains increased from 29% to 38% as the extrusion temperature was

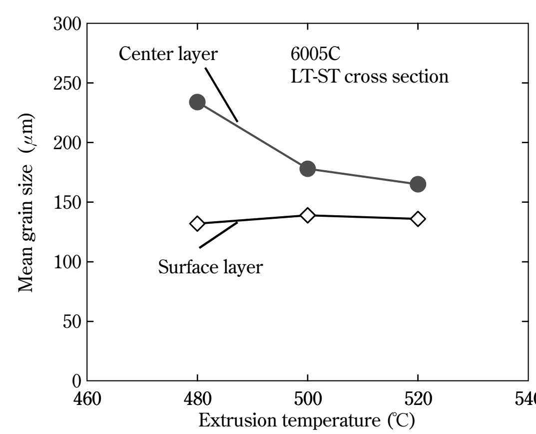

Fig. 5 Relationship of extrusion temperature and recrystallized grain size

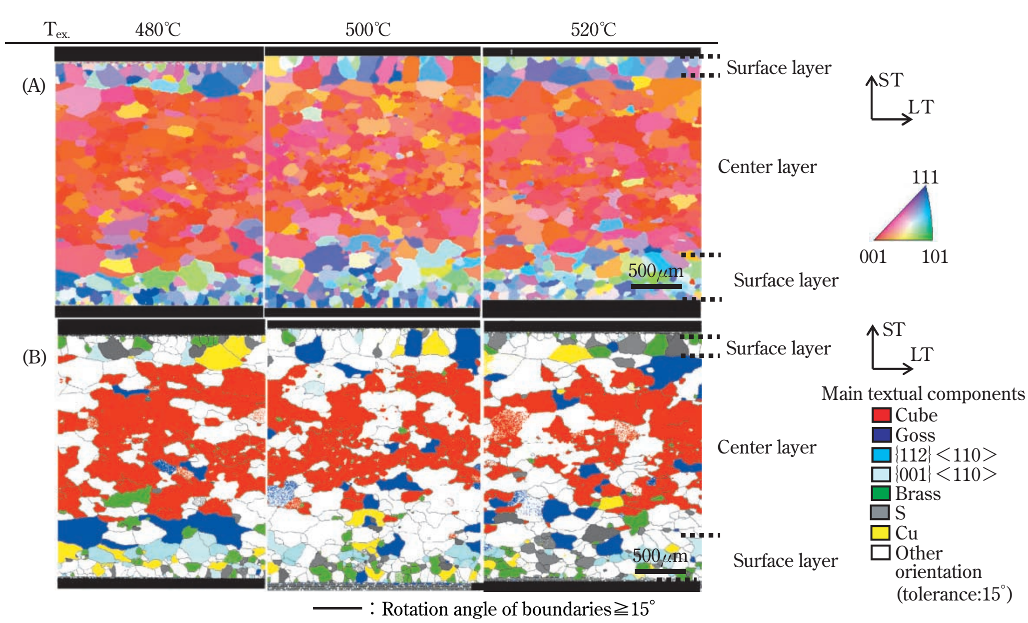

Fig. 4 SEM-EBSD maps of extruded 6005C-T5 alloys (A: Orientation distribution, B: Main textual components)

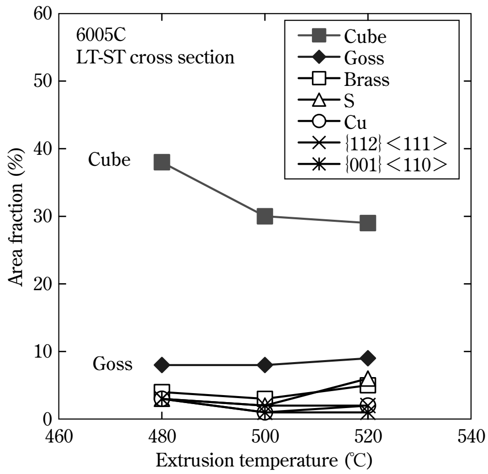

Fig. 6 Relation between area fraction of textual components and extrusion temperature

lowered from 520℃ to 480℃. The coarsening of the recrystallization grains in the center layer, which is due to the lowered extrusion temperature, corresponds to the increase in the area fraction of the Cube-oriented grains. It has been reported that, in the case of extruded round bars of the 6063 alloy, lowering the extrusion temperature from 520℃ to 400℃ decreases the ratio of <100> fiber from 53% to 27% in the recrystallization texture at a working ratio of 92%[6]. A similar tendency has also been reported for the case of extruded round bars of pure aluminum, for which the extrusion temperature was lowered from 480℃ to 290℃[7]. These studies include the temperature range in which the materials are not fully recrystallized with a significant amount of <111> fiber structure still remaining. Therefore, these results cannot be compared with the results of the present study, in which a fully recrystallized sample shows a tendency for the area fraction of the Cube-oriented grains to increase from 30% to 40% as the extrusion temperature is lowered from 520℃ to 480℃.

The area fractions of the major oriented grains, other than the Cube-oriented grains, remained almost unchanged regardless of the extrusion temperature. As the extrusion temperature increases, the area fraction of the Cube-oriented grain decreases. On the other hand, the total area fraction of the other oriented grains, excluding the major oriented grains measured, has increased. This implies that the higher extrusion temperature facilitates the recrystallization and growth of the grains having various orientations. It is reported that, in the case of rolled sheets, the bendability improves with the increase of the Cube-oriented grains[8), 9)]. To confirm this, a bending test according to the V-block method (JIS Z2248) was conducted in the LT direction of the samples. The result shows that

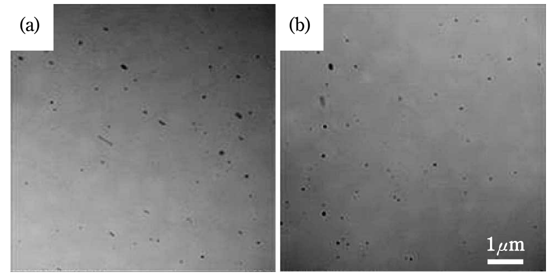

Fig. 7 Dispersoids in 6005C alloys extruded at (a)480℃, (b)520℃

decreasing the extrusion temperature from 520℃ to 480℃ decreases the critical bending radius from 1.5mm to 0.3mm, indicating that the higher the area fraction of the Cube-oriented grains, the better the bendability.

2.2.3 Dispersoids

Fig. 7 shows the TEM micrographs of the dispersoids in the samples extruded at the different temperatures. Both samples were homogenized at 520℃ for 4h, and almost no difference was found in the particle size and spacing of the Al-Fe-Si dispersoids. Thus, the dispersoids are not the cause of the increasing recrystallized grain size and the increasing area fraction of the Cube-oriented grain that are observed with a decreasing extrusion temperature. Rather, the change in the recrystallized grain size and texture is attributable to the extrusion temperature.

3. Discussion

3.1 Deformation temperature and the amount of accumulated strain

In order to clarify the recrystallization process of the samples, the microstructure of each sample was observed in the early stage of recrystallization during the elevated temperature compression test. **Fig. 8** shows the stress-strain curve. It is known that the deformation stress during elevated temperature

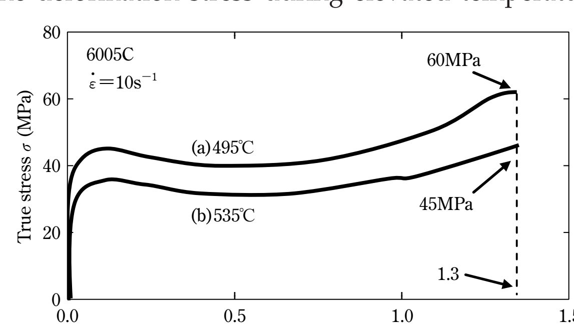

Fig. 8 Stress-strain curves for 6005C alloys compressed at (a)495℃, (b)535℃

deformation is proportional to the 1/2 power of the dislocation density, as in the case of ambient temperature deformation[10]. In the case of the present compression test, the material deformed at 495℃ exhibits a deformation stress approximately 30% greater than that of the material deformed at 535℃, indicating that its dislocation density is approximately 70% higher.

3.2 The crystal grain structure in the early stage of recrystallization

Fig. 9 shows the optical micrographs in the centers of the samples at 2 and 5 seconds have elapsed after they were compressively deformed for 75% at 535℃ and 495℃. When 2 seconds have elapsed, crystal grains having diameters of approximately 10 to 20μm are observed in the deformation structures, elongating in the transverse direction, for both the sample deformed at 535℃ and the one deformed at 495℃. These crystal grains are considered to be recrystallized grains because they are equiaxed. At the point where 5 seconds have elapsed, both of the samples, deformed at 535℃ and 495℃, exhibit the propagation of recrystallization throughout the region observed, with the growth of the recrystallized grains. The sample deformed at 495℃ exhibits a recrystallized grain size after the grain growth that is larger than that for the sample deformed at 535℃.

3.3 The crystal orientation distribution in the early stage of recrystallization

In order to confirm the formation of preferential orientation in the early stage of recrystallization, an SEM-EBSD analysis was conducted at the center of each of the samples 2 seconds after it had been compressively deformed. The results are shown in **Fig.10**. Fig.10 (a) shows the inverse pole figure maps in the compression axis direction with the orientations

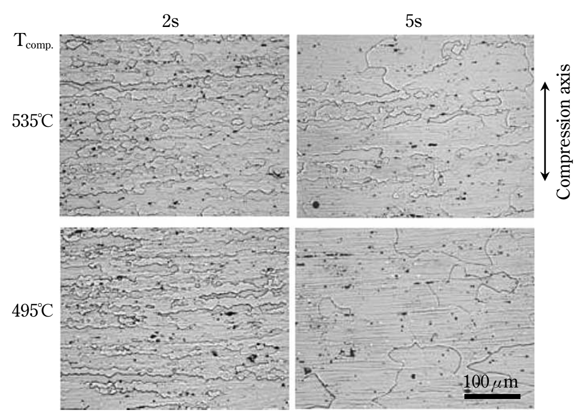

Fig. 9 Optical microstructure in center of compressed 6005C alloys

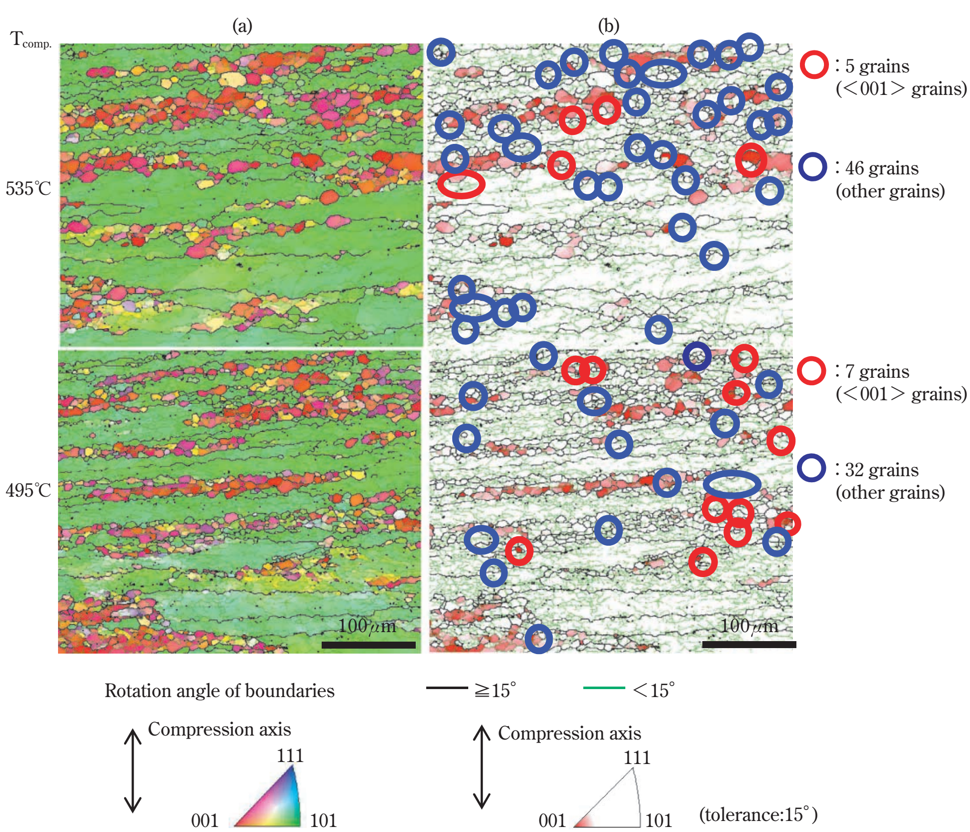

Fig.10 SEM-EBSD maps in center of compressed 6005C alloys
(a) orientation distribution of compression axis, (b) distribution of <001> grain

depicted by the color in the stereographic triangle below. The red region in the map is the area where the compression axis direction is oriented in the <001> direction, while the green region is the area where the compression axis direction is oriented in the <110> direction. The grains in these areas are herein referred to as "<001> grains" and "<110> grains", respectively. In Fig.10 (b), only the <001> grains are shown in red (tolerance: 15°), in which the black lines correspond to high-angle grain boundaries and the green lines to low-angle grain boundaries. The equiaxed crystal grains, surrounded by high-angle grain boundaries, but not including a low-angle grain boundary inside, are regarded as recrystallized grains. Among these recrystallized grains, the <001> grains are surrounded by red circles, while grains other than the <001> grains are surrounded by blue circles. The number of recrystallized grains in the measured field was found to be 51 for the sample deformed at 535℃ and 39 for the sample deformed at 495℃. Thus, the sample deformed at 495℃ has fewer recrystallized grains. The number of <001> grains was found to be 5 for the sample deformed at 535℃ and 7 for the sample deformed at 495℃. Thus the sample deformed at 495℃ has a higher ratio of <001> grains in the recrystallized grains.

3.4 The mechanism for the preferential growth of Cube orientation grains in the sample

The <110> orientation is considered to have a large Taylor factor for compressive deformation and a greater accumulated energy, while <100> is the orientation with a small Taylor factor for compressive deformation and has a smaller accumulated energy[11]. Therefore, the <001> grains shown in Fig.10 are considered to have an orientation that easily recovers and preferentially grows, the orientation which corresponds to the Cube-oriented in the center layer of the extruded material. The material deformed at 495℃ has fewer recrystallized grains, in the early stage of recrystallization, than the material deformed at 535℃ and has a larger ratio of <001> grains. In addition, the material deformed at 495℃ has a greater accumulation of strain energy in the un-recrystallized region, which increases the growth rate of the <001> grains that can preferentially grow. This is considered to result in the increased area fraction of the recrystallized grains, such as Cube-oriented grains, that can preferentially grow.

A phenomenon similar to that observed for the above described material that is compressively deformed at elevated temperatures is considered to be occurring in the extruded samples. **Fig.11** schematically illustrates the phenomenon. When the extrusion temperature is as low as 480℃, the number of recrystallized grains immediately after the deformation is small. However, the occupation rate of the Cube-oriented grains, which can easily recover, is considered to be high. In the un-recrystallized region, where there is a large accumulation of strain energy, the Cube-oriented grains, having a high growth rate, grow preferentially, increasing the area fraction of the Cube-oriented grains in the recrystallization structure after extrusion.

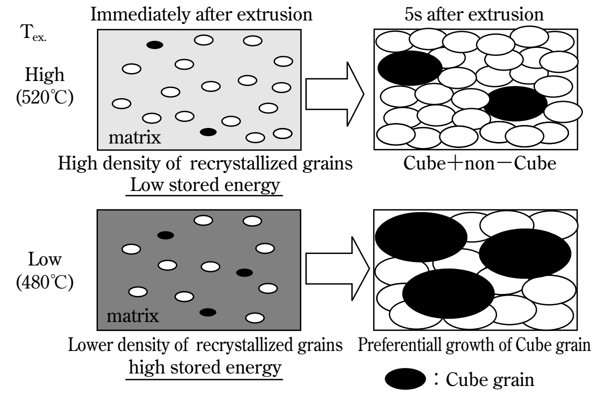

Fig.11 Schematic view of recrystallization in 6005C alloy

Conclusions

The change in recrystallization texture was studied in the T5 treated hollow profiles of a 6005C aluminum alloy, while lowering the extrusion temperature from 520℃ to 480℃. Elevated temperature compression tests were also performed to clarify the recrystallization process. The following conclusions were drawn:

- By lowering the extrusion temperature from 520℃ to 480℃, the average size of recrystallized grains increased from approximately 170 μm to approximately 230 μm, with the occupancy rate of the Cube-oriented grains increased from approximately 30% to approximately 40%.
- When the extrusion temperature is as low as 480℃, the number of recrystallized grains immediately after the deformation is small. However, the ratio of the Cube-oriented grains, which can easily recover, is considered to be large. This is considered to indicate that, in the un-recrystallized region, where there is a large accumulation of strain energy, the Cube-oriented grains, having a higher growth rate, grow preferentially, increasing the area fraction of the Cube-oriented grains in the recrystallization structure after extrusion.

References

1) T. Aiura et al. *KOBE STEEL ENGINEERING REPORTS*. 2002, Vol.52, No.3, p.83.
2) T. Furu et al. *Mater. Sci*. For. 519-521, 2006, 1421.
3) H. Inoue. *Journal of Japan Institute of Light Metals.* 2002, Vol.52, No.11, p.525.
4) J. Baumgarten et al. *Z.Metallkd*, 72 (1981), 162.
5) J. Baumgarten et al. *Z.Metallkd*. 72 (1981), 75.
6) T. Takahashi et al. *Journal of Japan Institute of Light Metals.* 1969, Vol.19, No.1, p.17.
7) J. Grewen et al. *Metall.* 12 (1959), 523.
8) S. Ikawa et al. *Journal of Japan Institute of Light Metals.* 2011, Vol.61, No.2, p.53.
9) A. Hibino et al. *Proceedings of the Japan Institute of Light Metals, 106th Spring Conference.* 2004, p.89.
10) F. R. Castro-Fernandes et al. Mats. Sci. and Tech. 6 (1990), 453.
11) H. Jeong et al. *Journal of Japan Institute of Light Metals*, 52 (2002), 525.
12) Japan Aluminium Association. *Aluminum Handbook 7th edition*. 2007, p.49.